Dynamics of CRISPR/Cas9-mediated genomic editing of the *AXL* locus in hepatocellular carcinoma cells

IRENE SCHARF, LISA BIERBAUMER, HEIDEMARIE HUBER, PHILIPP WITTMANN, CHRISTINE HAIDER, CHRISTINE PIRKER, WALTER BERGER and WOLFGANG MIKULITS

Department of Medicine I, Institute of Cancer Research, Comprehensive Cancer Center, Medical University of Vienna, A-1090 Vienna, Austria

Received May 11, 2017; Accepted August 4, 2017

DOI: 10.3892/ol.2017.7605

Abstract. Genomic editing using the CRISPR/Cas9 technology allows selective interference with gene expression. With this method, a multitude of haploid and diploid cells from different organisms have been employed to successfully generate knockouts of genes coding for proteins or small RNAs. Yet, cancer cells exhibiting an aberrant ploidy are considered to be less accessible to CRISPR/Cas9-mediated genomic editing, as amplifications of the targeted gene locus could hamper its effectiveness. Here we examined the suitability of CRISPR/Cas9 to knockout the receptor tyrosine kinase Axl in the human hepatoma cell lines HLF and SNU449. The genomic editing events were validated in two single cell clones each from putative HLF and SNU449 knockout cells (HLF-Axl$^-$-1, HLF-Axl$^-$-2, SNU449-Axl$^-$-1, SNU449-Axl$^-$-2). Sequence analysis of respective *AXL* loci revealed one to six editing events in each individual Axl$^-$ clone. The majority of insertions and deletions in the *AXL* gene at exon 7/8 resulted in a frameshift and thus a premature stop in the coding region. However, one genomic editing event led to an insertion of two amino acids resulting in an altered protein sequence rather than in a frameshift in the *AXL* locus of the SNU449-Axl$^-$-1 cells. Notably, while no Axl protein expression could be detected by immunoblotting in all four cell clones, both expression of total Axl as well as release of soluble Axl into the supernatant was observed by ELISA in incompletely edited SNU449-Axl$^-$-1 cells. Importantly, a comparative genomic hybridization array revealed comparable genomic changes in Axl knockout cells as well as in cells expressing Cas9 nickase without guide RNAs in SNU449 and HLF cells, indicating vast alterations in genomic DNA triggered by nickase. Together, these data show that the dynamics of CRISPR/Cas9 may cause incomplete editing events in cancer cell lines, as gene copy numbers vary based on genomic heterogeneity.

Correspondence to: Professor Wolfgang Mikulits, Department of Medicine I, Institute of Cancer Research, Comprehensive Cancer Center, Medical University of Vienna, Borschke-Gasse 8A, A-1090 Vienna, Austria
E-mail: wolfgang.mikulits@meduniwien.ac.at

Abbreviations: aCGH, array comparative genomic hybridization; Cas9, CRISPR associated 9; CDS, coding sequence; CRISPR, clustered regularly interspaced short palindromic repeats; DSB, double-strand break; ELISA, enzyme-linked immunosorbent assay; gRNA, guide ribonucleic acid; HDR, homology-directed repair; HCC, hepatocellular carcinoma; InDels, insertions and deletions; NGS, next generation sequencing; NHEJ, non-homologous end joining; ORF, open reading frame; PCR, polymerase chain reaction; RNAi, ribonucleic acid interference; sAxl, soluble Axl; shRNA, small hairpin ribonucleic acid; siRNA, small interfering ribonucleic acid; SN, supernatant; TALEN, transcription activator-like effector nucleases

Key words: CRISPR/Cas9, hepatocellular carcinoma cell lines, polyploidy, heterogeneity, genomic editing

Introduction

Loss-of-function analysis is a crucial issue in reverse genetic studies. In the past decade, RNA interference (RNAi) has been widely used to knockdown gene expression (1,2). RNAi is based on the binding of small interfering (si)RNAs to target transcripts leading to either its degradation or its inhibition at the translational level. siRNAs are either transiently delivered to cells or stably produced from small hairpin (sh)RNAs that are transcribed by polymerase III promoters. Albeit both siRNAs and shRNAs allow specific silencing of target genes (3), knockdowns by RNAi are mostly incomplete, vary between experiments and have unpredictable off-target effects (4,5).

New technologies have recently become available to generate knockouts rather than knockdowns of target genes in cultured cells. Among those techniques are transcription activator-like effector nucleases (TALENs) that use a pair of artificial DNA-binding domains fused to the catalytic domain of restriction endonuclease FokI which causes a double-strand break (DSB) at the targeted genomic locus stimulating DNA repair (6,7). Yet, TALEN is labor-intensive and works with low efficiency (8).

A more recently discovered technique of genomic engineering is clustered regulatory interspaced short palindromic repeats (CRISPR)/CRISPR associated 9 (Cas9), which is a unique mechanism of bacteria and archea to protect

themselves against foreign DNA penetration (9). This prokaryotic system has been adapted using a Cas9 endonuclease from *Streptococcus pyrogenes* that is guided to the target sequence by a guide RNA (gRNA) chimera that includes a protospacer adjacent motif. To reduce off-target effects, a mutant Cas9 termed nickase can be used which requires a pair of gRNAs to introduce site-specific single strand breaks, called nicks, that are together equivalent to a DSB (10). Of note, the use of two gRNAs and the nickase doubles the number of bases that need to be specifically recognized at the target locus and thereby significantly increases specificity.

DSBs introduced by TALEN or CRISPR/Cas9 at the targeted genomic locus are either repaired by the error prone non-homologous end joining (NHEJ) or by homology-directed repair (HDR). NHEJ leads to small insertions or deletions (InDels) that can result in a knockout of gene function due to frameshift mutations (11). The co-delivery of locus-specific homology arms with the site-specific nuclease triggers HDR-mediated genetic alterations and allows efficient integration of transgenes into an endogenous gene locus. First proof-of-principle studies showed that Cas9 can be successfully targeted to endogenous genes in bacteria (12), human pluripotent stem cells (13), as well as in whole organisms such as zebrafish (14), yeast (15), fruit flies (16), mice (17), rats (18) and rabbits (19). In addition, a haploid human cell line named engineered-HAPloid cells has been generated by megabase-scale deletion using CRISPR/Cas9 (20).

An important step in the use of genomic editing techniques is the confirmation of the knockout events. To analyze the targeted genomic locus, the target sequence is amplified by PCR, subcloned into a plasmid vector and subjected to sequencing (21). Another approach uses direct sequencing of the PCR products and analysis by 'Tracking InDels by Decomposition' (TIDE) which quantifies the editing efficacy and identifies predominant types of InDels in the targeted pool of cells (22). Other methods analyzing the efficiency of the Cas9-mediated DNA cleavage include heteroduplex formation that is examined either by high resolution melting analysis, heteroduplex mobility assay or T7 endonuclease I cutting. Using these methods, the ratio of homo- to heteroduplexes can be determined in order to estimate the nuclease efficiency. However, the latter method fails to accurately detect InDels (23).

Contrary to applications of CRISPR/Cas9 in haploid or diploid cells, genomic editing is more challenging when applied to hyperdiploid genomes as in the case of most cancer cells. In particular, all functional copies of the target gene must be edited in cancer cell lines to accomplish a complete knockout situation (24). As NHEJ works in a random fashion, there may arise altered structures without gene inactivation along NHEJ repair events. These insufficient knockout events, often combined with cellular heterogeneity, enhance the probability to generate partial knockouts that still harbor alleles coding for functional gene products or gene products with altered functionality (24). Hence, the determination of target gene copy number and cellular heterogeneity is essential in cancer cell populations to allow generation of solid CRISPR/Cas9-mediated knockouts and to correctly interpret the subsequent confirmation of knockout events.

The increase in aberrant ploidy levels and karyotypic complexity correlates with the progression of tumor cells from a benign neoplasm to malignant cancer. Chromosomal abnormalities occur in 75% of blood cancers and in more than 90% of solid tumors including hepatocellular carcinoma (HCC) (25,26). The overexpression of the receptor tyrosine kinase Axl along with the release of soluble Axl (sAxl) was detected in HCC and correlated with poor survival of HCC patients (27,28). In this study, we have generated knockouts of Axl in hepatoma cell lines using NHEJ-mediated CRISPR/Cas9 knockout technology. Our data show the dynamics of CRISPR/Cas9-mediated editing of the *AXL* locus in hyperdiploid hepatoma cell lines and reveal the drawbacks of the CRISPR/Cas9 technique in cancer cells.

Materials and methods

Cell culture. The human hepatoma cell lines SNU449 and HLF were cultured in RPMI-1640 supplemented with 10% fetal calf serum (FCS; Sigma, St. Louis, MO, USA) and DMEM plus 10% FCS, respectively. All cells were kept at 37˚C and 5% CO_2 and routinely screened for the absence of mycoplasma. All hepatoma cell lines were validated by short tandem repeat analysis.

CRISPR/Cas9-mediated genomic editing of the AXL locus. The *AXL* gene was disrupted in hepatoma cell lines using the human Axl gRNA CRISPR lentivirus set (K0161411, ABM, Milton, Ontario, Canada). HLF and SNU449 cells were infected with ready-to-use lentiviral stocks. Two or 6 μl of the gRNA pair and 2 or 6 μl of Cas9 nickase-encoding virus were added in a ratio of 1:2 to the cells. The medium was exchanged with standard culture medium after overnight incubation and cells were selected for stable expression of Cas9 for at least one week with 1 μg/ml puromycin. Single cell clones were generated by limiting dilution in 96-well plates and expanded to 100 mm culture plates. The single cell clones were further processed for sequence analysis of the *AXL* locus.

Sequence analysis of the genomic AXL locus. The gRNA binding region was amplified by polymerase chain reaction (PCR), cloned into a pGEM-T easy vector (A1360; Promega Corp., Madison, WI, USA) and transformed into *E. coli* DH5α competent bacteria for blue-white screening. The plasmid DNA of 20 bacterial colonies was sequenced by Sanger method and analyzed for sequence variations in the gRNA binding region. Single cell clones showing InDels in all 20 colonies were considered to be Axl-deficient (Axl^-).

Western blot analysis. Immunoblotting was done as described previously (29). The antibodies used were anti-Axl, 1:1,000 (AF154; R&D Systems, Inc., Minneapolis, MN, USA) and anti-Actin, 1:2,500 (A2066; Sigma-Aldrich, St. Louis, MO, USA).

Enzyme-linked immunosorbent assay (ELISA). Soluble Axl (sAxl) levels were assessed by ELISA using the DuoSet ELISA Development System Human Axl (DY154; R&D Systems, Inc.) from supernatants (SNs) of HLF and SNU449 cells. $1.5x10^6$ HLF or $0.8x10^6$ SNU449 cells were each seeded on 60 mm tissue culture plates. 24 h after plating, the cells were incubated in serum-free medium for further 24 h. Whole-cell

lysates of the same cells were measured by ELISA using a protein concentration of 0.1 mg/ml. The samples of parental cells were measured in 1:10 and 1:20 dilutions. To ensure the detection of Axl in the knockout situation, the SNs and protein lysates of Axl$^-$ cells were measured undiluted and at a dilution of 1:5. The concentrations of sAxl and Axl were normalized to 1.0x10^6 cells. All values below the standard curve were considered as noise and were therefore excluded. A seven-point standard curve was generated for each plate and quantification was performed using GraphPad Prism 5.01 software (GraphPad Software, Inc., La Jolla, CA, USA).

Cell migration. Cells (1x10^6)were seeded in 6-well tissue culture plates. Cells were scratched with a sterile pipette tip to generate artificial wounds. Phase contrast images were taken using the microscope Nikon-Eclipse Ti-S (Nikon Corporation, Tokyo, Japan) to monitor wound closure. The second set of phase contrast images was taken after 24 h of migration. The area of migration into the artificial wound was analyzed using ImageJ 1.44p.

Array comparative genomic hybridization (aCGH). Genomic DNA was isolated from SNU449 and HLF hepatoma cells including parental cells, Axl$^-$ single cell clones and a control clones expressing nickase without gRNAs using the QIAamp DNA Blood Mini kit (Qiagen, Hilden, Germany) according to the manufacturer's protocol. Direct and indirect aCGH analyses were performed using human whole genome oligonucleotide-based microarrays (SNU449: Cancer Research Array + single nucleotide polymorphism, 2x400K; HLF: 4x44K; both arrays from Agilent Technologies, Inc., Santa Clara, CA, USA). Normal human male DNA (Agilent Technologies, Inc.) or parental SNU449-derived DNA were used as reference samples in case of direct and indirect aCGH experiments, respectively. Labeling and hybridization was carried out following the protocols provided by the manufacturer. Slides were scanned with a G2600D Microarray Scanner (Agilent Technologies, Inc.). Feature extraction and data analysis were performed using the Feature Extraction and Agilent Genomic Workbench software (Agilent Technologies, Inc.), respectively.

Statistics. Data were expressed as means ± standard deviations. The statistical significance of differences was evaluated using a one-way analysis of variance followed by a Tukey's post hoc test. $^*P<0.05$, $^{**}P<0.01$ and $^{***}P<0.005$ were considered to indicate a statistically significant difference.

Results

Sequence analysis of the AXL locus in CRISPR/Cas9-edited hepatoma cells. To address the role of Axl signaling in HCC cells, we aimed at generating Axl-deficient HLF and SNU449 hepatoma cells. Both HLF and SNU449 cells were previously shown to exhibit a hyperdiploid DNA status (30,31). To accomplish this task, we performed CRISPR/Cas9-mediated genomic editing using a pair of gRNAs targeting the genomic *AXL* locus together with the expression of nickase. Genomic editing was induced in exon 7 or 8 depending on the pair of gRNAs used (Fig. 1A). The genomic editing events of two single cell clones each from HLF and SNU449 cells were analyzed after PCR amplification of the *AXL* locus by sequencing of 20 bacterial colonies each. In HLF cells, a gRNA pair was used that binds to DNA in Exon 7 (Fig. 1A and B). By analyzing the two HLF single cell clones, the first supposed Axl-negative clone, designated HLF-Axl$^-$-1, showed one genomic editing event with one defined deletion (Fig. 1B). Sequencing of the second Axl$^-$ clone (HLF-Axl$^-$-2) revealed two genomic editing events corresponding to deletions of various lengths (Fig. 1B). In SNU449 cells, the used gRNA pair bound to exon 8 of the *AXL* gene (Fig. 1A and B). Notably, one Axl$^-$ clone (SNU449-Axl$^-$-1) showed five genomic editing events, where two events were deletions and the other three ones resulted in insertions (Fig. 1B). The second Axl$^-$ clone (SNU449-Axl$^-$-2) exhibited six different genomic editing events consisting of two deletions, two insertions and two events resulting in a combination of InDels (Fig. 1B). From these data we conclude that multiple genomic editing events occurred at the *AXL* loci that were differentially affected by independent gRNA/Cas9 complexes.

Mutations of the AXL locus in CRISPR/Cas9-edited cells. As a next step we addressed the question of the consequences of these genomic editing events on Axl protein expression. All InDels that are not a multiple of three resulted in frameshift mutations, and as a consequence in premature stops of translation (Table I). However, the genomic editing event not resulting in a frameshift and premature stop was editing event 3 of SNU449-Axl$^-$-1, where six basepairs were inserted into the genomic *AXL* locus, which resulted in an insertion of two amino acids in the extracellular domain of Axl (Fig. 1B, Table I). In summary, these data suggest that CRISPR/Cas9-mediated genomic editing may result in the expected protein deficiency (HLF-Axl$^-$-1, HLF-Axl$^-$-2 and SNU449-Axl$^-$-2) or in the incomplete knockout of the Axl protein expression based on a single allele editing event (SNU449-Axl$^-$-1).

Expression of Axl in CRISPR/Cas9-edited cells. We next performed western blot analysis to detect the effects of the genomic editing events on Axl protein expression. Interestingly, no protein expression was observed in each of the HLF-Axl$^-$ and SNU449-Axl$^-$ single cell clones as compared to the HLF and SNU449 parental cells (p) or control HLF and SNU449 cells (n) expressing nickase without gRNAs (Fig. 2A). Furthermore, enzyme-linked immunosorbent assays (ELISAs) were performed to detect very low levels of Axl protein expression that could not be detected by the less sensitive western blot analysis. Thereby, we measured both the cleaved extracellular domain of Axl, termed soluble Axl (sAxl) in supernatants (Fig. 2B) as well as the full length Axl receptor in protein lysates (total Axl; Fig. 2C). Most notably, while no protein expression was observed in HLF-Axl$^-$-1, Axl$^-$-2 and SNU449-Axl$^-$-2 cells, significant expression of sAxl and total Axl was detected in SNU449-Axl$^-$-1 cells. Axl expression in this single cell clone confirmed the incomplete knockout (Fig. 1B, Table I), resulting in a 4-fold reduced expression to 24.7% of combined Axl values (sAxl + total Axl) as compared to parental SNU449-p cells (Table II). Noteworthy, all other CRISPR/Cas9-edited HLF and SNU449 single cell clones displayed no Axl expression at all (HLF-Axl$^-$-2, and SNU449-Axl$^-$-2) or showed very low Axl levels that were

Table I. Genomic editing by CRISPR/Cas9 in HLF and SNU449 cells.

Cell type	Editing event	Insertion (bp)	Deletion (bp)	Effect on protein
HLF-Axl$^-$-1	Editing 1		10	Frameshift-premature stop
HLF-Axl$^-$-2	Editing 1		73	Frameshift-premature stop
	Editing 2		29	Frameshift-premature stop
SNU449-Axl$^-$-1	Editing 1		14	Frameshift-premature stop
	Editing 2		24+5	Frameshift-premature stop
	Editing 3	6		2 AA insertion
	Editing 4	37		Frameshift-premature stop
	Editing 5	95		Frameshift-premature stop
SNU449-Axl$^-$-2	Editing 1		19	Frameshift-premature stop
	Editing 2	7		Frameshift-premature stop
	Editing 3		7	Frameshift-premature stop
	Editing 4	77	2	Frameshift-premature stop
	Editing 5	49+3	1	Frameshift-premature stop
	Editing 6	176+9		Frameshift-premature stop

AA, amino acid; Axl$^-$, Axl knockout; bp, base pair; CRISPR, clustered regularly interspaced short palindromic repeat.

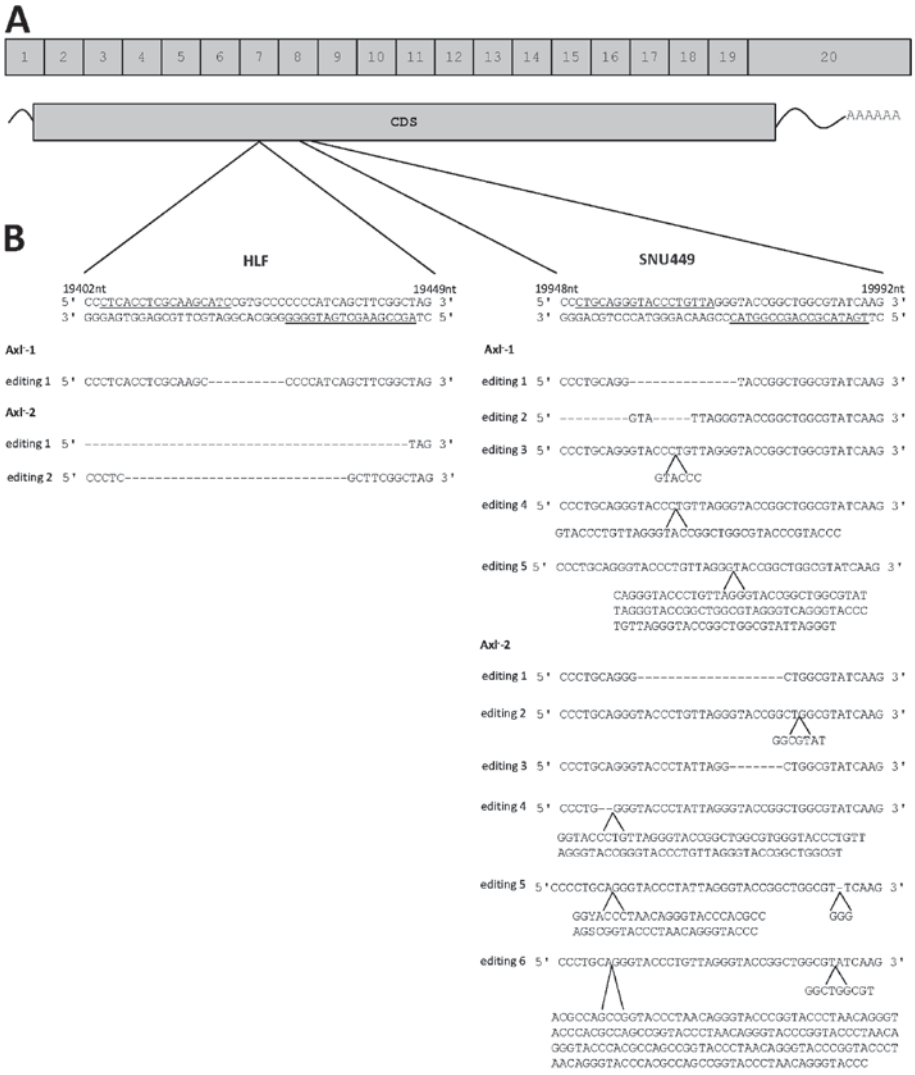

Figure 1. Genomic editing by CRISPR/Cas9 in HLF and SNU449 cells. (A) Grey boxes represent exons of the *AXL* gene locus. The CDS is indicated. (B) The genomic editing events in two clones of HLF (left panel; Axl$^-$-1, Axl$^-$-2) and SNU449 cells (right panel; Axl$^-$-1, Axl$^-$-2) are shown. The gRNA binding sites are underlined. All genomic editing events in the single cell clones are listed below the original sequence. CDS, coding sequence.

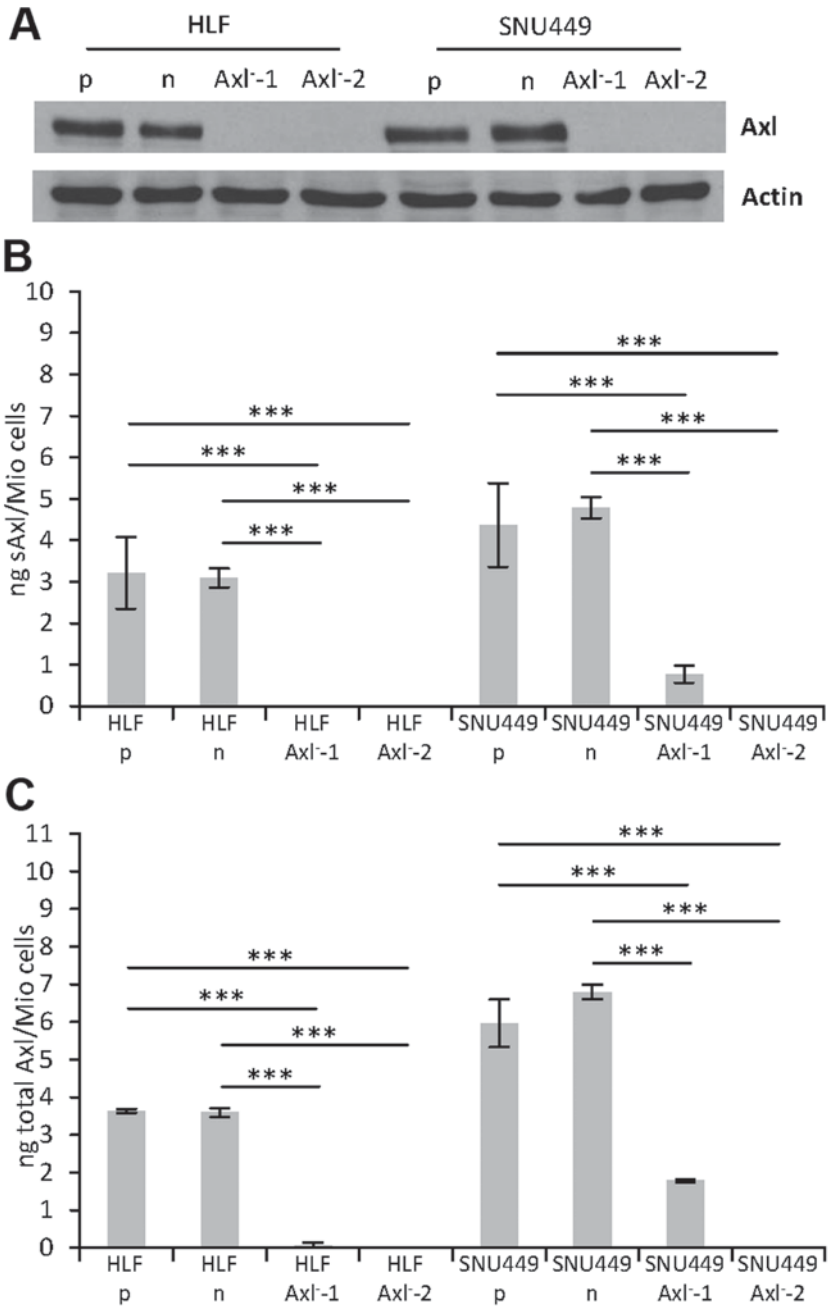

Figure 2. Expression of Axl protein in CRISPR/Cas9-edited hepatoma cells. (A) Western blot analysis of parental HLF and SNU449 cells as well as those expressing nickase without gRNAs (n) or nickase plus a pair of gRNAs as described in Fig. 1 (Axl$^-$-1, Axl$^-$-2). Actin is shown as a loading control. (B) Release of sAxl into cell supernatants of the same cells shown in (A) as determined by ELISA. sAxl protein was normalized to cell numbers. (C) Expression of total Axl as analyzed by ELISA of whole cell lysates. Total Axl protein was normalized to cell numbers. Two biological replicates were analyzed in triplicates by ELISA. Data are expressed as means ± standard deviations. ***P<0.0005. P, parental.

below the detection limit and thus considered as signal noise (HLF-Axl$^-$-1; Table II). Together, these data demonstrate that the genomic editing is incomplete in multi-allelic hepatoma cell lines, as three of four clones show deficiency of Axl and one clone maintains Axl expression despite genomic editing.

Migration of CRISPR/Cas9-edited hepatoma cells. Our recent data demonstrated that the siRNA-mediated loss of Axl expression caused a decrease of cell motility of human hepatoma cells (27). Therefore, we next analyzed the effects of the genomic editing events on the migratory cell behavior by performing a wound healing assay. A significant difference in migration was observed between the parental cells (p) or cells expressing nickase without gRNAs (n) and the Axl$^-$ clones in both, HLF and SNU449 cells (Fig. 3A and B). HLF-Axl$^-$-1 and HLF-Axl$^-$-2 cells showed comparable levels of migration which is around 40% reduced when compared to HLF-n or HLF-p cells. Interestingly, migration of SNU449-Axl$^-$-1 cells was reduced by approximately 20%, whereas SNU449-Axl$^-$-2 cells displayed half of the migration level of SNU449-n or SNU-449-p cells. In conclusion, the CRISPR/Cas9-edited hepatoma cells show a clear phenotype of diminished migration, thus confirming recent data obtained with siRNA. In addition, the incompletely edited SNU449-Axl$^-$-1 cells display an inhibition of migration

Table II. Axl protein levels in CRISPR/Cas9 edited HLF and SNU449 cells.

Cell type	sAxl (%)	Total Axl (%)	Combined Axl (%)
HLF-p	100	100	100
HLF-n	96.18	98.83	97.58
HLF-Axl$^-$-1	0	1.93	1.02
HLF-Axl$^-$-2	0	0	0
SNU449-p	100	100	100
SNU449-n	109.56	113.93	112.08
SNU449-Axl$^-$-1	17.66	29.88	24.7
SNU449-Axl$^-$-2	0	0	0

Axl, tyrosine-protein kinase receptor UFO; Axl$^-$, Axl knockout; n, nickase; p, parental; sAxl, soluble Axl; CRISPR, clustered regularly interspaced short palindromic repeat. Values given for HLF-n, HLF-Axl$^-$-1, HLF-Axl$^-$-2, SNU449-n, SNU449-Axl$^-$-1 and SNU449-Axl$^-$-2 cells are relative to parental cell lines.

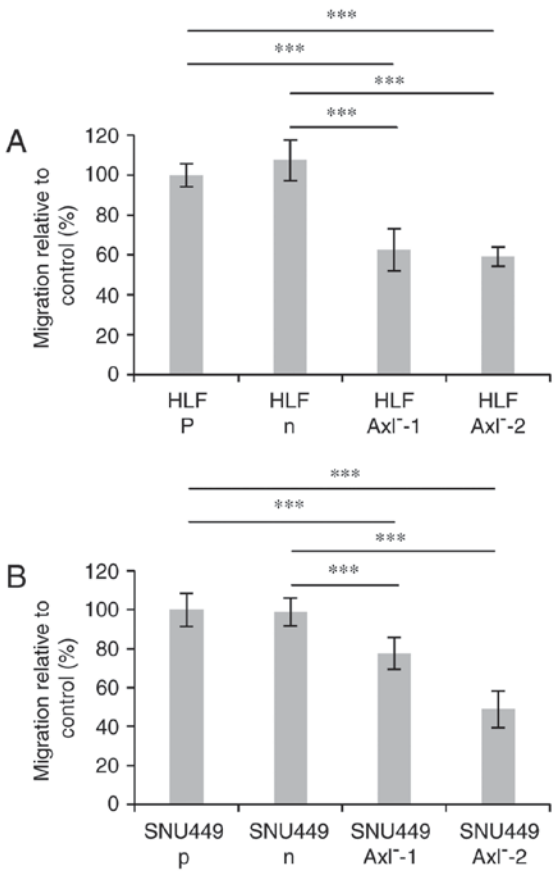

Figure 3. Migration of CRISPR/Cas9-edited hepatoma cells. (A) Migration of HLF parental (p), nickase (n), Axl$^-$-1 and Axl$^-$-2 cells. (B) Migration of SNU449 parental (p), nickase (n), Axl$^-$-1 and Axl$^-$-2 cells. Migration levels were normalized to migration of parental cells (100%). Data are expressed as means ± standard deviations. ***P-value <0.005.

with a lesser extent than those cells with a complete knockout (HLF-Axl$^-$, SNU449-Axl$^-$-2), indicating a close correlation between the genotype and the phenotype.

Genomic changes in CRISPR/Cas9-edited hepatoma cells. We further addressed the question on the gain and loss of genomic DNA in parental SNU449-p, control SNU449-n cells and SNU449-Axl$^-$ single cell clones by employing direct (SNU449-p) and indirect (control SNU449-n, SNU449-Axl$^-$-1, SNU449-Axl$^-$-2) array comparative genomic hybridization (aCGH) analyses. As expected, SNU449-p cells showed vast changes in genomic DNA as compared to the diploid reference DNA by multiple gains and losses (Fig. 4A). In more detail, these alterations included on the one hand focal deletions/amplifications such as e.g. deletions at chromosome 9p21 (CDKN2A) and 16q21 (CDH8, CDH11) and amplifications at 17p11.2 (MAPK7, MFAP4). On the other hand, these genomic changes involved gains and losses of whole chromosomes/chromosome arms such as loss of chromosome 3, loss of chromosome 7q, and gain of chromosome 10. Importantly, SNU449-n cells showed multiple differences in genomic DNA alterations as compared to SNU449-p cells (Fig. 4B, red line), suggesting that the constitutive expression of nickase induced changes in the genomic DNA despite the absence of gRNAs. A very similar pattern of genomic alterations was observed in both SNU449-Axl$^-$-1 and SNU449-Axl$^-$-2 cells expressing gRNAs (Fig. 4B, turquoise and blue lines, respectively), suggesting that a multitude of genomic changes in control SNU449-n, SNU449-Axl$^-$-1 and SNU449-Axl$^-$-2 cells is primarily caused by nickase activity.

SNU449-p cells showed a gain at the *AXL* locus with a mean $\log_2$ ratio of 0.3 (data not shown). SNU449-n, SNU449-Axl$^-$-1 and SNU449-Axl$^-$-2 cells each displayed an additional low level gain of chromosome 19q at the *AXL* locus (Fig. 4C). However, both SNU449-Axl$^-$-1 and SNU449-Axl$^-$-2 cells displayed the expected deletion of the *AXL* locus as a decrease in *AXL*-specific genomic DNA could be detected (Fig. 4C), thus confirming CRISPR/Cas9-specific genomic editing events. In particular, five and four *AXL*-specific oligonucleotides indicated a loss of genomic DNA in SNU449-Axl$^-$-1 and SNU449-Axl$^-$-2 cells between nucleotide 20198 and 21255 as well as 21179 and 22539 of the *AXL* gene, respectively. Both regions encompassing the *AXL*-specific oligonucleotides were located downstream of the gRNA binding sites.

We performed additional aCGH analyses of parental HLF cells, one HLF clone derived from nickase-treated cells and two Axl knockout clones. Comparable to the results obtained in SNU449 cells, parental HLF cells showed a multitude of gains and losses which is characteristic for cancer cells, thus mirroring a highly aberrant and re-arranged genome (Fig. 5A). In these cells as well, the chromosomal region 19q13.2 containing the *AXL* locus showed a low level gain (about 1.2-fold) as compared to normal diploid cells (data not shown). Interestingly, both Axl knockout clones as well as the clone derived from the nickase treated cells displayed various new, additional changes as compared to parental HLF cells (Fig. 5B). Together, these data provide evidence that high resolution aCGH detects CRISPR/Cas9-mediated genomic editing of *AXL*. Furthermore, the expression of nickase alone rather than the CRISPR/Cas9-dependent editing of the *AXL* locus causes pleiotropic gene-dose changes in the genome of established HCC cell lines.

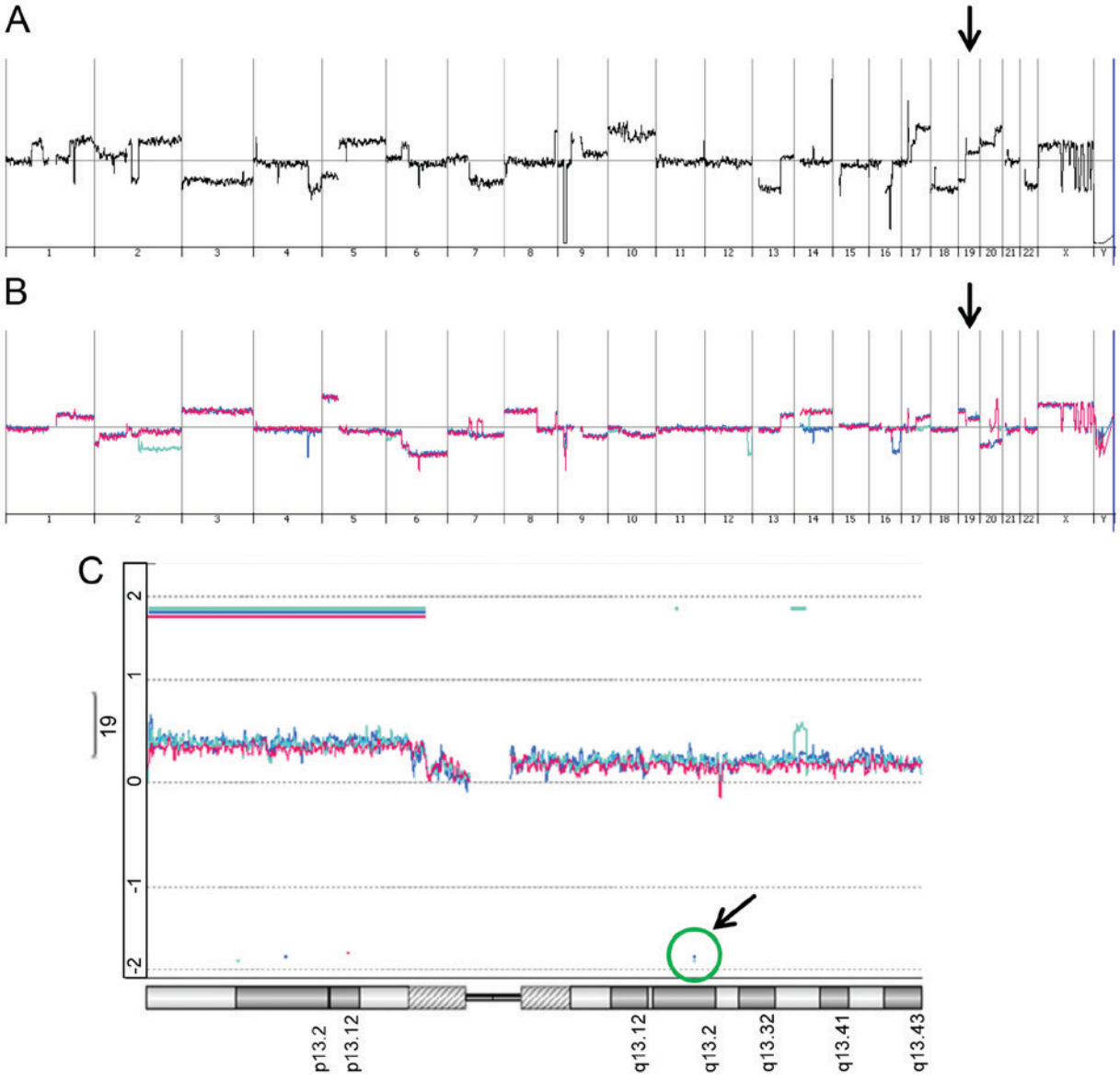

Figure 4. Changes in genomic DNA of SNU449 HCC cells subjected to CRISPR/Cas9-mediated editing of the *AXL* locus. aCGH analysis of parental SNU449 cells (SNU449-p) and those expressing either nickase without gRNAs (SNU449-n) or nickase plus gRNAs for the knockout of *AXL* (SNU449-Axl$^-$-1 and SNU449-Axl$^-$-2). (A) Gain and loss of genomic DNA in SNU449-p cells compared to diploid cells. (B) Comparison of genomic changes between control SNU449-n cells as well as SNU449-Axl$^-$-1 and SNU449-Axl$^-$-2 cells to SNU449-p cells. (C) Magnification of genomic changes in chromosome 19. The loss of the *AXL* locus in SNU449-Axl$^-$-1 and SNU449-Axl$^-$-2 cells at 19q is indicated by the green circle plus an arrow. The arrow in (A) and (B) indicates chromosome 19. Red line, SNU449-n; turquoise line, SNU449-Axl$^-$-1; blue line, SNU449-Axl$^-$-2 cells.

Discussion

Despite the extraordinary achievements of the CRISPR/Cas9 technology in genome engineering, its application still poses a challenging task in hyperdiploid cancer cell models. The data obtained in this study strongly suggest that ploidy and gene copy number play an important role in the efficacy of the CRISPR-dependent genomic editing. Two recent studies demonstrated that CRISPR/Cas9 is not suitable in cellular cancer models showing gene amplifications, as overrepresented genomic regions cause false positive results. Aguirre *et al* (32) provided evidence that DNA breaks generated by the CRISPR/Cas9 system lead to gene-independent cell toxicity and the number of DNA cuts rather than the gene knockout predicts the cellular response. Munoz *et al* (33) found a higher number of lethal genes when using CRISPR/Cas9 as compared to RNAi. In aneuploid cancer cell models, the genes located in amplified regions scored as lethal, indicating false positive results as already described by Aguirre *et al* (32). Thus, the number of loci representing the gene of interest in a cancer cell line under investigation is of crucial importance for the physiological response to CRISPR/Cas9 and for the experimental interpretation.

Established cancer cell lines frequently represent a pool of genetically heterogeneous subclones with varying numbers of chromosomes and different physiological behavior. These progressive genomic alterations and aneuploidy might drive a high degree of genomic instability leading to new mutations and gene-dose alterations over time and thus give rise to

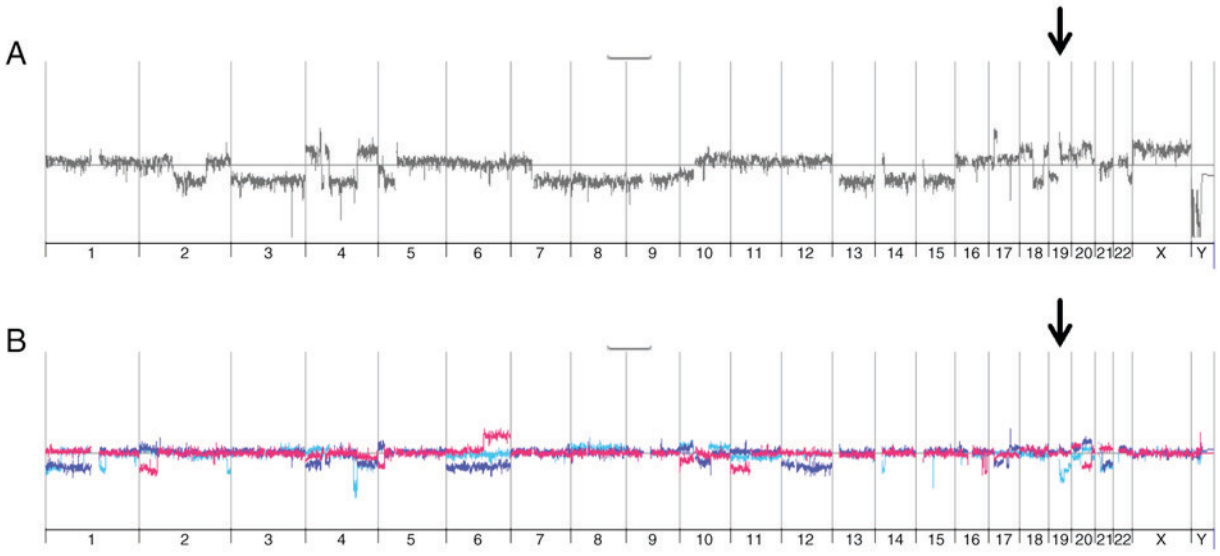

Figure 5. Changes in genomic DNA of HLF HCC cells subjected to CRISPR/Cas9-mediated editing of the *AXL* locus. aCGH analysis of parental HLF cells (HLF-p) and those expressing either nickase without gRNAs (HLF-n) or nickase plus gRNAs for the knockout of *AXL* (HLF-Axl^{-}-1 and HLF-Axl^{-}-2). (A) Gain and loss of genomic DNA in HLF-p cells compared to diploid cells. (B) Comparison of genomic changes between control HLF-n cells as well as HLF-Axl^{-}-1 and HLF-Axl^{-}-2 cells to HLF-p cells. The arrow in (A) and (B) indicates chromosome 19. Red line, HLF-n; turquoise line, HLF-Axl^{-}-1; blue line, HLF-Axl^{-}-2 cells.

new subclones (34). The predominance of such subclones can change depending on time and conditions of cultivation. Upon selection of CRISPR/Cas9-positive cells, expansion of single cells harbor the risk of developing a phenotype not specific for the knockout as cells go through multiple cell divisions in which compensatory mechanisms could arise due to the loss of the target protein. Even without any genetic manipulation, single cell clones can behave differently from the original cancer cell population and might not be representative for a certain cancer cell model. Thus, the use of CRISPR/Cas9 might have drawbacks in cancer cell lines as the reliable evaluation of experiments is less predictable in the absence of data about target gene copies and the dynamic modulation of subclone heterogeneity also under the stress of clonal selection.

Notably, the expression of nickase in the absence of gRNAs in SNU449 and HLF cells causes multiple genomic changes comparable to those in CRISPR/Cas9-processed cells in the presence of gRNAs (Figs. 4B and 5B). These data show that gRNA expression results in specific editing of the targeted *AXL* locus and further suggest that cells expressing nickase without gRNAs represent the most suitable control for CRISPR/Cas9-edited cells. In this context, however, it is an open issue whether the genomic changes observed in nickase-only expressing cells are due to the pleiotropic activity of nickase or due to the selection of a favorable subclone from heterogenous SNU449-p or HLF-p cells. Thus, further aCGH profiling of nickase-only expressing cells vs. representative subclones of parental hepatoma cells could clarify the impact of clonal selection vs. nickase activity and the evolution of genomic alterations as compared to the parental cell pool.

In order to reduce unspecific genomic changes by the nickase, CRISPR-Cas9 inhibitory proteins could be expressed to inhibit the activity of Cas9 after genomic editing (35,36). The prophage-encoded inhibitor proteins AcrIIA2 and AcrIIA4, which allow phages to evade the bacterial host's CRISPR/Cas immune system, were found to inhibit Cas9-based targeting in their native host *Listeria monocytogenes*, as well as Cas9 of *Streptococcus pyogenes* in bacteria and human cells. Another approach for minimizing off-target effects employs the delivery of Cas9 protein/gRNA ribonucleoprotein complexes (37). When delivering Cas9 protein directly, cleavage occurs only temporarily, as the Cas9 protein is rapidly degraded in cells (38).

The confirmation of the desired gene knockout requires the determination of target protein levels in a large number of single cell clones using immunoblotting and the more sensitive ELISA. Interestingly, this study showed different levels of Axl protein in SNU449-Axl^{-}-1 cells when detected either by immunoblotting or ELISA (Fig. 2), albeit the same polyclonal Axl-specific antibody was employed in both methods. We speculate that the insertion of two additional amino acids into the *AXL* locus of CRISPR/Cas9-edited SNU449-Axl^{-}-1 cells (Fig. 1B, Table I) accounts for changes in the protein structure or the stability of the Axl protein allowing detection in its native form by ELISA but no detection of the reduced form by immunoblotting. Obviously one incompletely edited copy of *AXL* was enough to produce considerable amount of protein that is detectable by ELISA. In accordance with these data, both SNU449-Axl^{-} clones exhibited a significant reduction of the migratory phenotype, which was less pronounced in incompletely edited SNU449-Axl^{-}-1 cells (Fig. 3).

Furthermore, 20 bacterial colonies of the *AXL*-specific PCR-amplified region were each analyzed by sequencing in order to verify the complete knockout. As 20 analyses might not cover all genomic changes, we suggest applying next generation sequencing (NGS) methods to identify all InDels in the targeted gene locus. NGS analysis could be even employed at various passage numbers during selection

in order to examine the dynamics of subclonal evolution. In case of many alleles and an incomplete knockout, one intact and functional target gene copy, even if not detected in the beginning, could provide a particular growth advantage in culture over time.

Loss-of-function studies employing CRISPR/Cas9, TALEN or stable RNAi involve selection of edited cells through multiple cell divisions in which compensatory mechanisms could arise due to the loss/knockdown of the target protein, resulting in altered cellular phenotypes. Notably, transient RNAi by siRNA transfection could overcome such drawbacks as cells are not subjected to selection and might not adapt to environmental conditions. Thus, siRNA-induced changes are more likely due to the downregulation of the target protein rather than to an artifact derived from clonal selection. Since transient RNAi is only used for short-term analysis, we suggest to compare e.g. the CRISPR/Cas9 phenotype with the one obtained by transient RNAi, both of which must coincide in phenotypical characteristics *in vitro*.

In conclusion, the CRISPR/Cas9 system has the advantage of generating a complete and stable knockout which can be successfully used in cancer cell lines by considering the above mentioned aspects. Once the knockout is confirmed and selection artefacts can be excluded, a robust and trustworthy system has been established.

Acknowledgements

The present study was supported by the Austrian Science Fund, FWF, P25356 and the Herzfelder Family Foundation.

References

1. Davidson BL and Paulson HL: Molecular medicine for the brain: Silencing of disease genes with RNA interference. Lancet Neurol 3: 145-149, 2004.
2. Xia H, Mao Q, Paulson HL and Davidson BL: siRNA-mediated gene silencing in vitro and in vivo. Nat Biotechnol 20: 1006-1010, 2002.
3. Miller VM, Xia H, Marrs GL, Gouvion CM, Lee G, Davidson BL and Paulson HL: Allele-specific silencing of dominant disease genes. Proc Natl Acad Sci USA 100: 7195-7200, 2003.
4. Gaj T, Gersbach CA, Barbas CF III: ZFN, TALEN, and CRISPR/Cas-based methods for genome engineering. Trends Biotechnol 31: 397-405, 2013.
5. Liberali P, Snijder B and Pelkmans L: Single-cell and multivariate approaches in genetic perturbation screens. Nat Rev Genet 16: 18-32, 2015.
6. Joung JK and Sander JD: TALENs: A widely applicable technology for targeted genome editing. Nat Rev Mol Cell Biol 14: 49-55, 2013.
7. Miller JC, Tan S, Qiao G, Barlow KA, Wang J, Xia DF, Meng X, Paschon DE, Leung E, Hinkley SJ, *et al*: A TALE nuclease architecture for efficient genome editing. Nat Biotechnol 29: 143-148, 2011.
8. Harrison MM, Jenkins BV, O'Connor-Giles KM and Wildonger J: A CRISPR view of development. Genes Dev 28: 1859-1872, 2014.
9. Jinek M, Chylinski K, Fonfara I, Hauer M, Doudna JA and Charpentier E: A programmable dual-RNA-guided DNA endonuclease in adaptive bacterial immunity. Science 337: 816-821, 2012.
10. Hryhorowicz M, Lipinski D, Zeyland J and Slomski R: CRISPR/Cas9 immune system as a tool for genome engineering. Arch Immunol Ther Exp (Warsz) 65: 233-240, 2017.
11. Lopes R, Korkmaz G and Agami R: Applying CRISPR-Cas9 tools to identify and characterize transcriptional enhancers. Nat Rev Mol Cell Biol 17: 597-604, 2016.
12. Jiang W, Bikard D, Cox D, Zhang F and Marraffini LA: RNA-guided editing of bacterial genomes using CRISPR-Cas systems. Nat Biotechnol 31: 233-239, 2013.
13. Mali P, Yang L, Esvelt KM, Aach J, Guell M, DiCarlo JE, Norville JE and Church GM: RNA-guided human genome engineering via Cas9. Science 339: 823-826, 2013.
14. Hwang WY, Fu Y, Reyon D, Maeder ML, Tsai SQ, Sander JD, Peterson RT, Yeh JR and Joung JK: Efficient genome editing in zebrafish using a CRISPR-Cas system. Nat Biotechnol 31: 227-229, 2013.
15. DiCarlo JE, Norville JE, Mali P, Rios X, Aach J and Church GM: Genome engineering in Saccharomyces cerevisiae using CRISPR-Cas systems. Nucleic Acids Res 41: 4336-4343, 2013.
16. Bassett AR, Tibbit C, Ponting CP and Liu JL: Highly efficient targeted mutagenesis of Drosophila with the CRISPR/Cas9 system. Cell Rep 4: 220-228, 2013.
17. Wang H, Yang H, Shivalila CS, Dawlaty MM, Cheng AW, Zhang F and Jaenisch R: One-step generation of mice carrying mutations in multiple genes by CRISPR/Cas-mediated genome engineering. Cell 153: 910-918, 2013.
18. Li D, Qiu Z, Shao Y, Chen Y, Guan Y, Liu M, Li Y, Gao N, Wang L, Lu X, *et al*: Heritable gene targeting in the mouse and rat using a CRISPR-Cas system. Nat Biotechnol 31: 681-683, 2013.
19. Yang D, Xu J, Zhu T, Fan J, Lai L, Zhang J and Chen YE: Effective gene targeting in rabbits using RNA-guided Cas9 nucleases. J Mol Cell Biol 6: 97-99, 2014.
20. Essletzbichler P, Konopka T, Santoro F, Chen D, Gapp BV, Kralovics R, Brummelkamp TR, Nijman SM and Bürckstümmer T: Megabase-scale deletion using CRISPR/Cas9 to generate a fully haploid human cell line. Genome Res 24: 2059-2065, 2014.
21. Ran FA, Hsu PD, Wright J, Agarwala V, Scott DA and Zhang F: Genome engineering using the CRISPR-Cas9 system. Nat Protoc 8: 2281-2308, 2013.
22. Brinkman EK, Chen T, Amendola M and van Steensel B: Easy quantitative assessment of genome editing by sequence trace decomposition. Nucleic Acids Res 42: e168, 2014.
23. Nemudryi AA, Valetdinova KR, Medvedev SP and Zakian SM: TALEN and CRISPR/Cas genome editing systems: Tools of discovery. Acta Naturae 6: 19-40, 2014.
24. Boettcher M and McManus MT: Choosing the right tool for the job: RNAi, TALEN, or CRISPR. Mol Cell 58: 575-585, 2015.
25. Roschke AV and Rozenblum E: Multi-layered cancer chromosomal instability phenotype. Front Oncol 3: 302, 2013.
26. Teoh NC, Dan YY, Swisshelm K, Lehman S, Wright JH, Haque J, Gu Y and Fausto N: Defective DNA strand break repair causes chromosomal instability and accelerates liver carcinogenesis in mice. Hepatology 47: 2078-2088, 2008.
27. Reichl P, Dengler M, van Zijl F, Huber H, Führlinger G, Reichel C, Sieghart W, Peck-Radosavljevic M, Grubinger M, Mikulits W, *et al*: Axl activates autocrine transforming growth factor-β signaling in hepatocellular carcinoma. Hepatology 61: 930-941, 2015.
28. Reichl P, Fang M, Starlinger P, Staufer K, Nenutil R, Muller P, Greplova K, Valik D, Dooley S, Brostjan C, *et al*: Multicenter analysis of soluble Axl reveals diagnostic value for very early stage hepatocellular carcinoma. Int J Cancer 137: 385-394, 2015.
29. Petz M, Them N, Huber H, Beug H and Mikulits W: La enhances IRES-mediated translation of laminin B1 during malignant epithelial to mesenchymal transition. Nucleic Acids Res 40: 290-302, 2012.
30. Hwang HJ, Kim GJ, Lee GB, Oh JT, Chun YH and Park SH: A comprehensive karyotypic analysis on Korean hepatocellular carcinoma cell lines by cross-species color banding and comparative genomic hybridization. Cancer Genet Cytogenet 141: 128-137, 2003.
31. Dor I, Namba M and Sato J: Establishment and some biological characteristics of human hepatoma cell lines. Gan 66: 385-392, 1975.
32. Aguirre AJ, Meyers RM, Weir BA, Vazquez F, Zhang CZ, Ben-David U, Cook A, Ha G, Harrington WF, Doshi MB, *et al*: Genomic copy number dictates a gene-independent cell response to CRISPR/Cas9 targeting. Cancer Discov 6: 914-929, 2016.
33. Munoz DM, Cassiani PJ, Li L, Billy E, Korn JM, Jones MD, Golji J, Ruddy DA, Yu K, McAllister G, *et al*: CRISPR screens provide a comprehensive assessment of cancer vulnerabilities but generate false-positive hits for highly amplified genomic regions. Cancer Discov 6: 900-913, 2016.

34. Hastings RJ and Franks LM: Cellular heterogeneity in a tissue culture cell line derived from a human bladder carcinoma. Br J Cancer 47: 233-244, 1983.
35. Rauch BJ, Silvis MR, Hultquist JF, Waters CS, McGregor MJ, Krogan NJ and Bondy-Denomy J: Inhibition of CRISPR-Cas9 with bacteriophage proteins. Cell 168 150-158.e110, 2017.
36. Pawluk A, Amrani N, Zhang Y, Garcia B, Hidalgo-Reyes Y, Lee J, Edraki A, Shah M, Sontheimer EJ, Maxwell KL and Davidson AR: Naturally occurring off-switches for CRISPR-Cas9. Cell 167: 1829-1838.e9, 2016.
37. Liang X, Potter J, Kumar S, Zou Y, Quintanilla R, Sridharan M, Carte J, Chen W, Roark N and Ranganathan S: Rapid and highly efficient mammalian cell engineering via Cas9 protein transfection. J Biotechnol 208: 44-53, 2015.
38. Kim S, Kim D, Cho SW, Kim J and Kim JS: Highly efficient RNA-guided genome editing in human cells via delivery of purified Cas9 ribonucleoproteins. Genome Res 24: 1012-1019, 2014.